Bull. Mater. Sci., Vol. 5, Nos 3 & 4, August & October 1983, pp. 247–256.

The Verwey transition

C M SRIVASTAVA

Department of Physics and Advanced Centre for Research in Electronics, Indian Institute of Technology, Bombay 400076, India

Abstract. The origin of Verwey transition in magnetite is investigated. It is shown that the transport properties in the high temperature phase of magnetite can be accounted by a phonon-induced correlated electron transfer mechanism. Assuming that the condensation of this phonon mode leads to Verwey transition, the isotope and pressure effects have been explained. The electron energy band diagram consistent with the electrical transport behaviour in the low temperature phase has been constructed.

Keywords. Verwey transition; magnetite; transport properties; electron energy band.

1. Introduction

The low temperature phase of magnetite below the Verwey transition temperature, T_v, has been the subject of extensive investigations (Weiss and Forrer 1929; Li 1932; Verwey and Haaymaan 1941; Verwey *et al* 1947). Mössbauer (Ito *et al* 1963; Hargrove and Kundig 1970; Robinstein and Forester 1971; Iida *et al* 1977; Rosenberg and Franke 1980; Srivastava *et al* 1981), NMR (Iida *et al* 1978; Mizoguchi and Tomono 1966; Boyd 1963), x-ray (Kobayashi *et al* 1963; Yoshida and Iida 1979; Iida *et al* 1980), neutron diffraction (Samuelson *et al* 1968; Shirane *et al* 1975), electrical transport (Calhoun 1954; Miles *et al* 1957; Matsui *et al* 1977a), magnetic (Bickford *et al* 1957; Abe *et al* 1976; Matsui *et al* 1977b) and thermal (Matsui *et al* 1977a) properties have been investigated for this phase on single and polycrystalline samples of magnetite. However, studies on the basic mechanism responsible for this transition are meagre. Various suggestions that the electronic state at T_v, undergoes Mott transition, Wigner crystallisation or Anderson localisation have been made but the matter is still unsettled (Goodenough 1982; Mott 1980).

The Verwey transition is characterised by a sharp rise in conductivity at T_v by two orders of magnitude from about 0·5 $(\Omega-\text{cm})^{-1}$ to 40 $(\Omega-\text{cm})^{-1}$ and a crystal symmetry change from monoclinic below T_v to cubic above T_v. Based on the results of the diffraction and resonance experiments many models for the structure of the low-temperature phase have been proposed. We describe briefly some of these models. The Verwey model (Verwey and Haaymaan 1941) assumes that below T_v, the Fe^{2+} and Fe^{3+} ions on B sites arrange on linear chains alternately along the [110] and [1$\bar{1}$0] directions of the cubic phase respectively. Since neutron diffraction experiments indicate a long range order with equal number of Fe^{2+} and Fe^{3+} ions on (001) planes, the Verwey model is inapplicable. The Yamada model (Yamada 1975) attempts to explain the observed doubling of the unit cell in the low temperature phase. The monoclinic unit cell has the dimension, $\sqrt{2}\,a_0 \times \sqrt{2}\,a_0 \times 2a_0$, where a_0 is the cell constant of the cubic phase. Yamada suggested that Fe^{2+} and Fe^{3+} alternated along the [1$\bar{1}$0] direction or the a-axis and this ordering reversed itself from one a-axis to the

next along the c-axis. This explains the existence of the $(h, k, l \pm 1/2)$ spots observed in the electron (Yamada *et al* 1968) and neutron (Fuji *et al* 1975) diffraction experiments. The atoms on the [110] or the b-axis are, however, not allowed to order in this model. A model of complete ordering has been put forward on the basis of NMR and Mössbauer spectra by Mizoguchi (1978) and Iida *et al* (1978). The model has been refined by Iida (1980) and has been made consistent with most of the known experimental data. The relevant feature of this model is the existence of a unit hexagon network of six-B-site ions which are alternately Fe^{2+} and Fe^{3+}. As pointed out by Cullen (1980) the configurational free energy of this unit is small and makes it strongly susceptible to charge fluctuations which destroy part of the long-range order and explains the partial ordering in the C_a plane only.

The theory of Verwey transition has been discussed by Mott (1974, 1980), Cullen and Cullen (1971, 1973), Sakoloff (1976), Ihle and Lorenz (1980) and Chakravorty (1980). These theories qualitatively explain some of the experimental data but none of these is entirely satisfactory. A critical review of these theories is given by Mott (1980).

Recently, it was shown (Srinivasan and Srivastava 1981) that the conductivity in the high temperature phase of magnetite can be satisfactorily accounted by a phonon-induced correlated electron transfer mechanism. It is shown that the system consisting of equal numbers of Fe^{2+} and Fe^{3+} ions located alternately on a linear chain on the edge shared octahedra, through coupling with a longitudinal optic phonon mode, oscillates between two degenerate states and thereby lowers the energy of the system. The condensation of this phonon mode is assumed to lead to the Verwey transition. Based on this assumption the isotope and pressure effects on the Verwey temperature have been satisfactorily explained (Srivastava 1983). This paper reviews this theory and uses it to explain some more experimental data on the low temperature phase of magnetite.

2. Correlated electron transfer mechanism and the electrical conductivity

Consider a linear chain on which Fe^{2+}, Fe^{3+} and oxygen ions are arranged respectively at sites, $r_{N\pm 4n}$, $r_{N+2\pm 4n}$ and $r_{N+1\pm 2n}$ where $0 \leqslant n \leqslant \infty$ and describe it as ψ_{I}. Another state ψ_{II} in which the Fe^{2+} and Fe^{3+} ions are interchanged is degenerate with ψ_{I} for a static lattice but the degeneracy is lifted in the presence of phonons. The phonon coupled ψ_{I} and ψ_{II} states obey the Schrödinger equation (Srinivasan and Srivastava 1981)

$$\left.\begin{aligned} \frac{\mathrm{d}\psi_{\mathrm{I}}}{\mathrm{d}t} &= -\frac{i}{\hbar}(\mu\psi_{\mathrm{I}} + \varepsilon\psi_{\mathrm{II}}), \\ \frac{\mathrm{d}\psi_{\mathrm{II}}}{\mathrm{d}t} &= -\frac{i}{\hbar}(\mu\psi_{\mathrm{II}} + \varepsilon\psi_{\mathrm{I}}). \end{aligned}\right\} \tag{1}$$

Here μ is the small polaron stabilisation energy and ε is the phonon energy. Describing the probability of excitation of carriers by the random-walk probability expression

$$f_+ - f_- = \frac{2}{[\exp(\beta\mu/2) + \exp(-\beta\mu/2)]^2} \tag{2}$$

derived from a one-dimensional function

$$f_\pm = \frac{(\beta eEl)^{-1}\exp\{\beta/2(\mu + eEl)\}}{\exp\{\beta/2(\mu \pm eEl)\} + \exp\{-\beta/2(\mu \pm eEl)\}}, \tag{3}$$

the conductivity is given by (Srinivasan and Srivastava 1981)

$$\sigma = (f_+ - f_-)2N_0 e^2 l^2 \beta E/\hbar. \tag{4}$$

Here E is the external field, l is the nearest neighbour jump distance, $\beta = 1/k_B T$ and N_0 is the number of charge carriers. Using $N_0 = 1{\cdot}36 \times 10^{28}\ \mathrm{m}^{-3}$, $l = 2{\cdot}963$ Å, $\varepsilon/h = 1{\cdot}37 \times 10^{12}$ Hz, $\mu = 0{\cdot}055$ eV in (4) we obtain a good fit for the variation of σ with T in magnetite with the data of Miles *et al* (1957) and Kupiers and Brabers (1976) in the temperature region $T_v < T < 300$ K. The conductivity data in the high temperature phase are thus consistent with the concept of a localised down spin electron that hops between nearest-neighbour sites but without any activation enthalpy ($\Delta H_m = 0$) due to coupling with a longitudinal optic phonon.

3. Isotope effect

The isotope effect on the Verwey temperature has been studied by Terukov *et al* (1979). They find that T_v increases with the increase in the isotopic mass of the oxygen ion.

It is natural to assume that the correlated electron transfer exists only when a certain minimum amplitude of vibration is exceeded. This minimum is obtained at T_v. Below T_v the mode freezes giving a static deformation. Consider now the mean-square amplitude of vibration $\langle \delta R_i^2 \rangle$ at a given temperature and assume that

$$\gamma = \langle \delta R_i^2 \rangle / R_0^2 \tag{5}$$

has a minimum value γ_v at T_v. Here R_0 is the internuclear distance between the metal and oxygen ions on the B-sites. For a phonon mode of wavevector k and polarization λ, in usual notation,

$$\langle \delta R_i^2 \rangle = \frac{1}{MN} \langle q_{k\lambda}^+ q_{k\lambda} \rangle, \tag{6}$$

where,

$$q_{k\lambda} = (\hbar/2w_k)^{1/2} (a_{k\lambda} + a_{-k\lambda}^+). \tag{7}$$

So

$$\langle \delta R_i^2 \rangle = \frac{1}{MN} \frac{\langle E_{k\lambda} \rangle}{w_{k\lambda}^2}. \tag{8}$$

For N oscillators in one dimension all having the same frequency, w_0,

$$\langle E_{k\lambda} \rangle = N\hbar w_0 \{ \langle n_0 \rangle + 1/2 \}, \tag{9}$$

Hence from (5), (8) and (9)

$$\gamma_v = \frac{1}{M} \frac{\hbar}{w_0 R_0^2} \left\{ \frac{1}{\exp(\beta_v \hbar w_0) - 1} + \frac{1}{2} \right\}. \tag{10}$$

The conductivity data (§2) yields the phonon frequency $\nu_0 = 1{\cdot}37 \times 10^{12}$ Hz, so for $T_v = 120$ K, $\beta_v \hbar w_0 = 0{\cdot}55$. In the first approximation we may then replace $\exp(\beta_v \hbar w_0)$ by $1 + \beta_v \hbar w_0 + (\beta_v \hbar w_0)^2/2$ which reproduces the value of the exponential to the first decimal place. We then have

$$\begin{aligned} \gamma_v &= \frac{1}{M} \frac{\hbar}{w_0 R_0^2} \left\{ \frac{1}{\beta_v \hbar w_0} \left(1 + \frac{\beta_v \hbar w_0}{2} \right)^{-1} + \frac{1}{2} \right\} \\ &\simeq \frac{1}{M} \frac{k_B T_v}{w_0^2 R_0^2}. \end{aligned} \tag{11}$$

The vibrations of the longitudinal optic phonon mode could be visualised as shown in figure 1. In the first half of the vibration the oxygen ions indicated by the open circles move towards the *B* site Fe ions on alternate sites located on the linear chain of the edge shared octahedra. During the second half they move towards the other site. This leads to the polaron stabilisation energy $\mu = 0{\cdot}055$ eV discussed above. This vibration can be decomposed in terms of the vibrations of a triatomic molecule with a stationary central atom of mass m and two identical masses moving in opposite phases. The analysis of this mode (Goldstein 1970) leads to the eigenfrequency, w_0, of $(C/M)^{1/2}$ and the eigenvector proportional to $(2M)^{-1/2}$ where C is the force constant.

This suggests that

$$\gamma_v = \xi M = \frac{k_B T_v}{M w_0^2 R_0^2} = \frac{k_B T_v}{C R_0^2}, \tag{12}$$

where ξ is a constant. From (12) we have

$$\Delta T_v / T_v = \Delta M / M. \tag{13}$$

For 43% ^{18}O substitution for ^{16}O in Fe_3O_4, we obtain from (13), $\Delta T_v = 6{\cdot}4$ K for $T_v = 119$ K. This compares favourably with the observed value of $(6{\cdot}1 \pm 0{\cdot}05)$ K (Terukov *et al* 1979).

4. Pressure effect

The application of pressure decreases the Verwey temperature (Samara 1968; Kakudate *et al* 1979). This follows from (12),

$$\frac{dT_v}{dp} = \frac{2\gamma_v M R_0 w_0}{k_B}\left[R_0 \frac{dw_0}{dp} + w_0 \frac{dR_0}{dp}\right]. \tag{14}$$

Now,

$$dR_0/dp = -\beta R_0/3, \tag{15}$$

and

$$\frac{dw_0}{dp} = \frac{dw_0}{dv}\frac{dv}{dp} = (w_0 r_G/v)(-\beta v) = -\beta w_0 \gamma_G, \tag{16}$$

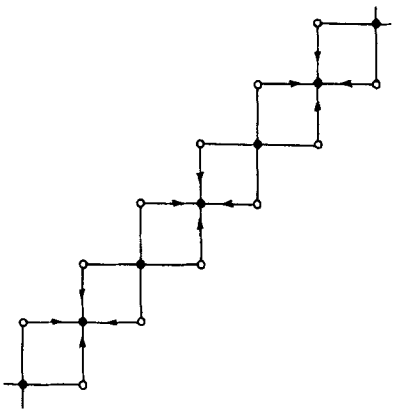

Figure 1. The active longitudinal optic mode of vibration responsible for the correlated electron transfer mechanism on the octahedral metal sites.

where γ_G is the Grüneisen constant and β is the compressibility. From (12), (14), (15) and (16),

$$dT_v/dp = -2T_v\beta(\gamma_G + 1/3). \tag{17}$$

The pressure dependence of Verwey temperature is thus directly proportional to T_v. The dT_v/dp for the two samples of Fe_3O_4 with T_v equal to 120 K and 112 K have been found (Samara 1968) to be $-(0{\cdot}48 \pm 0{\cdot}02)$ K/kbar and $-(0{\cdot}44 \pm 0{\cdot}02)$ K/kbar respectively. The experimental ratio of dT_v/dp for these two samples is 1·09. This compares favourably with the theoretical ratio of 1·07 given by (17).

The Grüneisen constant of magnetite has not been reported. Using the dT_v/dp and T_v values given above and taking $\beta = 0{\cdot}56 \times 10^{-12}$ cm^{2}dyne^{-1} we obtain a value of 3·19 for γ_G which is reasonable (Srivastava 1983).

Kakudate *et al* (1979) found that in the high temperature phase the temperature of the conductivity maximum, T_M, decreases with pressure more rapidly than the Verwey temperature, T_v. Working with synthetic single crystal of magnetite, they have found $dT_M/dp = -4{\cdot}1$ K/kbar and $dT_v/dp = -0{\cdot}27$ K/kbar. The latter is smaller than the value obtained by Samara (1968). Kakudate *et al* (1979) attribute it to the difference between the synthetic and natural single crystals used in the two studies. From (4) the temperature of the conductivity maximum, T_M, satisfies the equation

$$\exp\beta_M\mu = (\beta_M{}^{\mu+1})/(\beta_M{}^{\mu-1}), \tag{18}$$

where $\beta_M = 1/k_BT_M$. A graphical solution of (18) yields $\beta_M\mu = 1{\cdot}55$. Thus

$$T_M = \mu/1{\cdot}55\,k_B. \tag{19}$$

Using $\mu = 0{\cdot}055$ eV we obtain $T_M = 411$ K which is about 20% higher than the observed value (Samara 1968; Kakudate *et al* 1979).

From (19)

$$dT_M/dp = (1/1{\cdot}55\,k_B)\,(d\mu/dp). \tag{20}$$

It is expected that the small polaron stabilisation energy will decrease with pressure so the observed decrease of T_M with p can be explained. Using the above value for dT_M/dp we obtain $-0{\cdot}35$ MeV/kbar for $d\mu/dp$.

5. Seebeck coefficient

For small polaron, the Seebeck coefficient, S, is given by

$$S = -k_B/e\,[\ln\beta\,\{(1-c)/c\} + S_T^*/k_B]. \tag{21}$$

Here β is the spin degeneracy, S_T^* is the entropy of the transport term, c is the fraction of conduction sites of lower valence. The Seebeck coefficient in the high temperature phase of magnetite has been measured by Whall *et al* 1977 and Wu and Mason (1981).

The term S_T^*/k_B in magnetite is small, of the order of 10 μV/K, and can be neglected (Wu and Mason 1981). The statistical term in the high temperature phase represents a few problems. The experimental data (Whall *et al*1977) shows that as the temperature is increased above T_v, S gradually increases in magnitude from about -50 μV/K at 120 K to -60 μV/K at 600 K and then rises rapidly to -85 μV/K at $T_N = 850$ K. There on the value increases gradually to -120 μV/K at about 1500 K (Wu and Mason 1981). This is shown in figure 2.

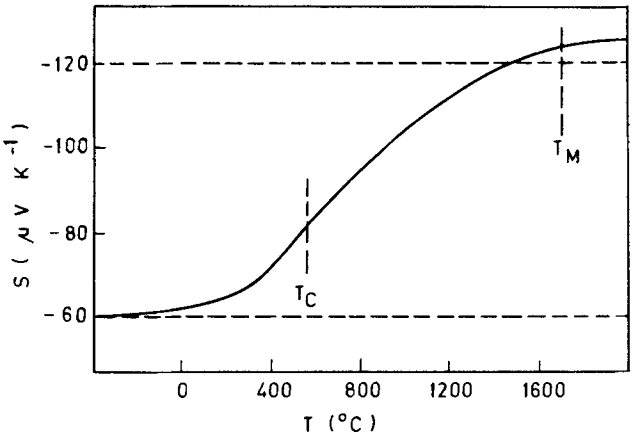

Figure 2. Thermoelectric power for the high temperature phase of magnetite (Wu and Mason 1981).

For $T \ll T_N$, $\beta = 1$ and for magnetite, c is expected to be 1/2 which would make the statistical term in S vanish in (21). On the other hand the chemical substitution of magnetite has shown that the room temperature data on S for mixed ferrites can be fitted to (Srinivasan and Srivastava 1981)

$$S = -\frac{k_B}{e}\ln(1/c). \tag{22}$$

For $c = 1/2$, (22) yields a value of $-60\ \mu$V/K and hence this expression also satisfies the data on magnetite in the temperature range $T_v < T < 300$ K. It thus appears that the correlated electron transfer mechanism is responsible for the change in the expression of the statistical term from (21)–(22).

In the very high temperature limit ($T \gg T_N$) the correlation disappears and the hopping electron jumps to the A site. In this case c becomes 1/3, $\beta = 2$ and (21) is applicable. Substituting these values we obtain $S = -120\ \mu$V/K, which is in agreement with experiment.

In the low temperature phase ($T < T_v$) the Seebeck coefficient shows complex behaviour (Kupiers and Brabers 1976; Graener *et al* 1979). At T_v, S increases in magnitude from $-60\ \mu$V/K to $-120\ \mu$V/K when the sample is cooled from the high to low temperature side of T_v. As the sample is cooled further the magnitude decreases rapidly, changes sign (figure 3), reaches a maximum of $+50\ \mu$V/K at about 75 K and then drops rapidly to $-90\ \mu$V/K at about 50 K.

The explanation offered by Kupiers and Brabers (1976) on the basis of a two-level model serves to explain only the initial part of the thermopower curve. The expression for thermoelectric power in the presence of both hole and electronic type of charge carriers is

$$S = \frac{1}{eT}\frac{-n(\Delta - E_F) + p(\Delta + E_F)\mu_p/\mu_n}{n + p\mu_p/\mu_n}, \tag{23}$$

where 2Δ is the energy gap between the two levels, E_F is the Fermi energy, n and p are the concentrations of the electronic and hole types of charge carriers and μ_n and μ_p are their

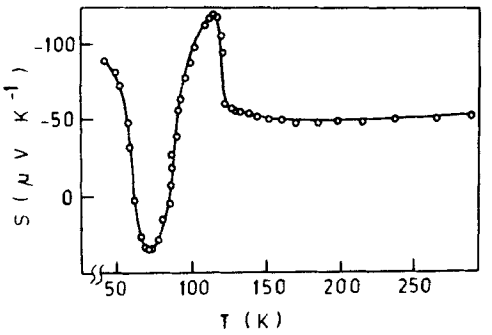

Figure 3. Thermoelectric power for the low temperature phase of magnetite (Graener *et al* 1979).

mobilities. Although this expression diverges as $T \rightarrow 0$, it fits the data in the temperature range of 90 K and T_v. This emphasises the need to study the electron energy band diagram of magnetite.

Goodenough (1982) has constructed a semiempirical energy band diagram for magnetite at room temperature (figure 4) which is based on the optical spectrum of Schlegel *et al* (1979), the polarised-spin UV photoelectron-spectroscopy measurements of Alvarado *et al* (1976) and some other observations. The general features of the diagram are (i) the Fermi energy is 3·8 eV above the top of the O^{2-}: $2p^6$ band, (ii) the crystal field splitting for the *A* and *B* sites are 1 and 2 eV respectively, (iii) the trigonal field at the *B* site splits the t_{2g} levels in a singlet (*a*) and a doublet (*e*) levels, (iv) the Fe^{3+}/Fe^{2+} redox band for the *A* ions lies on energy Δ above E_F and is empty, while for the *B* ions it is split into a partially occupied *a* (↓) and *e* (↓) bands, (v) the 4*s* band lies 3·2 eV above E_F. The arrows indicate the spin direction of the magnetically ordered state.

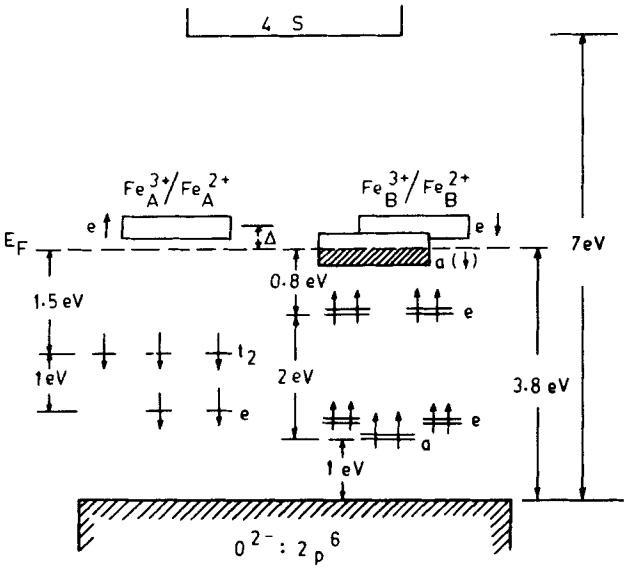

Figure 4. Electron energy band diaram of magnetite at room temperature (Goodenough 1982).

In the low temperature phase the energy band is modified due to the change from a higher symmetric cubic phase to a lower symmetric monoclinic phase. As discussed above, the change occurs due to the freezing of the longitudinal optical phonon mode. The active optical vibration interacts with electrons in the band and changes the electronic structure. The interaction also leads to a change in the frequency of the interacting optical phonon. It can be shown that if there are two neighbouring energy bands in the higher symmetry phase, one of which is completely occupied and the other completely empty, the width of the forbidden band, E_g, in the lower symmetry phase is temperature dependent and is given by (Fridkin 1980)

$$E_g = 2\left[-\frac{1}{4}E_{g0}^2 + \frac{V^2}{N}u_0^2(T)\right]^{1/2}, \tag{24}$$

where E_{g0} is the energy gap in the higher symmetric phase, V is the interaction constant of the interband electron-phonon interaction, N is the number of electrons in the lower band and $u_0(T)$ is the amplitude of the active phonon mode at temperature T.

The Mössbauer and NMR data indicate that Fe^{2+} and Fe^{3+} ions on the B-site on the Ca and Cb planes are not in the same electronic states below T_v. The hyperfine field of Fe^{2+}(I) is 489 kOe while for the other Fe^{2+}(II) it is 365 kOe (Srivastava *et al* 1981). There are five different types of Fe^{3+} B-sites (Iida 1980) but for simplicity we consider only two Fe^{3+}(I) and Fe^{3+}(II). The semiempirical energy diagram for the low temperature phase is given in figure 5. This is based on our analysis of the Mössbauer data and the wave functions deduced for the Fe^{2+}(I) and Fe^{2+}(II) states (Srivastava *et al* 1981). The Fe^{2+}(II) has a larger covalency contribution so the splitting Δ_2 is higher compared to Δ_1 for Fe^{2+}(I). The electron on Fe^{2+}(II) is also more localised so the separation between $a(\downarrow)$ levels of Fe^{2+}(II) and Fe^{3+}(II) is larger than E_{g0}, the energy gap between the a_1 ($\downarrow$) bands of Fe^{2+}(I) and Fe^{3+}(I). States I are treated as narrow bands while states II are considered to be localised levels.

At T_v the energy gap, E_{g0}, will have a minimum, since the amplitude of the active phonon mode $u_0(T_v)$ vanishes. As the temperature is lowered $u_0(T)$ increases and hence E_g increases. It is now easy to understand the behaviour of Seebeck coefficient. At T_v, the electrons from the lower band Fe^{2+}(I): $a_1(\downarrow)$ are excited to Fe^{3+}(I): $a(\downarrow)$ in large numbers as E_{g0} is small. As the temperature is decreased, E_{g0} increases and a number of electrons drop to the lower level, so S becomes positive and the model of Kupiers and

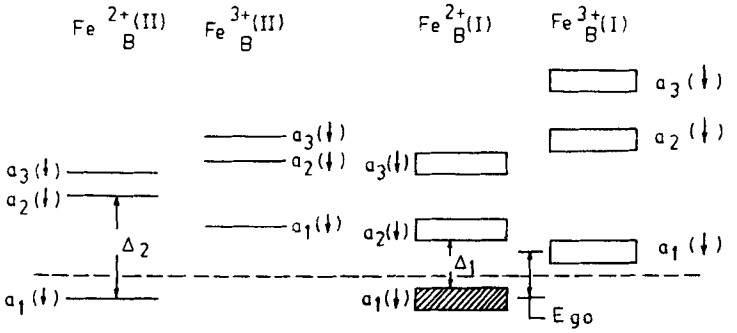

Figure 5. Splitting of Fe^{3+}/Fe^{2+} redox bands for $T < T_v$ in the monoclinic phase of magnetite for the B site ions.

Brabers (1976) holds in this region. As the temperature is further decreased, on account of a high energy gap, most of the electrons are in Fe^{2+}: $a_1(\downarrow)$ band and the conduction is by the diffusion mechanism making the Seebeck coefficient change from the positive to the negative sign.

It is found that small presence of impurity (Kupiers and Brabers 1976) or small flourine substitution for oxygen (Graener *et al* 1979) drastically changes the positive peak of S. If there is excess of Fe^{2+} ions, the extra electrons will try to fill Fe^{2+} (I): $a_2(\downarrow)$ band, so there will always be a large number of electrons in the conduction band and hence the hole contribution will not be observed. The energy diagram thus explains qualitatively the salient features of Seebeck coefficient.

6. Conclusion

An attempt has been made to explain the complex electrical transport properties of magnetite above and below the Verwey transition on the basis of the electron-phonon interaction. The model also explains the isotope and pressure effects on Verwey transition temperature. The electron energy diagram in the low temperature phase has been constructed and is found to be consistent with the data on Seebeck effect.

References

Abe K, Miyamoto Y and Chikazumi S 1976 *J. Phys. Soc. Jpn.* **41** 1894
Alvarado S F, Erbudak M and Munz P 1976 *Phys. Rev.* **B14** 2740
Bickford Jr L R, Brownlow J M and Penoyer R F 1957 *Proc. Inst. Elec. Engrs. Suppl. No. 5* **B104** 238
Boyd E L 1963 *Phys. Rev.* **129** 1962
Calhoun B A 1954 *Phys. Rev.* **94** 1577
Chakravorty B K 1980 *Philos. Mag.* **B42** 473
Cullen J R 1980 *Philos. Mag.* **B42** 387
Cullen J R and Cullen E R 1971 *Phys. Rev. Lett.* **26** 236
Cullen J R and Cullen E R 1973 *Phys. Rev.* **B7** 397
Fridkin V M 1980 *Ferroelectric semiconductors* (New York: Consultants Bureau) p. 32
Fujii Y, Shirane G and Yamada Y 1975 *Phys. Rev.* **B11** 2036
Goldstein H 1970 *Classical mechanics* (New Delhi: India Book Co.) pp. 333
Goodenough J B 1982 invited talk presented at the Seminar on *Recent Advances in Materials Research* held at I.I.T Bombay, India Dec. 20–22 1982 to be published by Oxford and IBH Co. New Delhi
Graener H, Rosenberg M, Whall T E and Jones M R S 1979 *Philos. Mag.* **B40** 389
Hargrove R S and Kundig W 1970 *Solid State Commun.* **8** 303
Ito A, Ono K and Ishikawa Y 1963 *J. Phys. Soc. Jpn* **18** 1468
Ihle D and Lorenz B 1980 *Philos. Mag.* **B42** 337
Iida S, Mizushima K, Mizoguchi M, Mada J, Umemura S, Yoshida J and Nakao K 1977 *J. Phys. (Paris)* **38** C1–73
Iida S, Mizushima K, Mizoguchi M, Umemura S and Yoshida J 1978 *J. Appl. Phys.* **49** 1455
Iida S 1980 *Philos. Mag.* **B42** 349
Iida S, Mizoguchi M, Umemura S, Yoshida J, Kato K and Yanai K 1980 *J. Appl. Phys.* **50** 7584
Kabayashi J, Yamada N and Nakamura T 1963 *Phys. Rev. Lett.* **11** 410
Kakudate Y, Mori N and Koni Y 1979 *J. Magn. Magn. Mater.* **12** 22
Kupiers A J M and Brabers V A M 1976 *Phys. Rev.* **B14** 1401
Li C H 1932 *Phys. Rev.* **40** 1002
Matsui M, Todo S and Chikazumi S 1977a *J. Phys. Soc. Jpn.* **42** 1517
Matsui M, Todo S and Chikazumi S 1977b *J. Phys. Soc. Jpn.* **43** 47
Miles P A, Westphal W B and Von Hippal A 1957 *Rev. Mod. Phys.* **29** 279
Mizoguchi M 1978 *J. Phys. Soc. Jpn* **44** 1501, 1512

Mizoguchi T and Tomono Y 1966 *J. Phys. Soc. Jpn.* **36** 1021
Mott N F 1974 *Metal-insulator transitions* (London: Taylor and Francis Ltd.)
Mott N F 1980 *Philos. Mag.* **B42** 327
Robinstein M and Forester D W 1971 *Solid State Commun.* **9** 1475
Rosenberg M and Franke H 1980 *Philos. Mag.* **B42** 419
Sakoloff J B 1976 *Phys. Rev.* **B13** 2003
Samara G D 1968 *Phys. Rev. Lett.* **21** 795
Samuelson E J, Bleeker E J, Dobrzynski L and Riste T 1968 *J. Appl. Phys.* **39** 1114
Schlegel A, Alvarado S F and Wachter P 1979 *J. Phys.* **40** C12–115
Shirane G, Chikazumi S, Akimitsu J, Chiba K, Matsui M and Fujii Y 1975 *J. Phys. Soc. Jpn.* **39** 949
Srinivasan G and Srivastava C M 1981 *Phys. Status Solidi* **B103** 665
Srivastava C M 1983 Isotope and pressure effects on the Verwey temperature of magnetite, *Phys. Lett.* (to appear)
Srivastava C M, Shringi S N and Babu M V 1981 *Phys. Status Solidi* **A65** 731
Terukov E I, Reichelt W, Ihle D and Oppermann H 1979 *Phys. Status Solidi* **B95** 491
Verwey E J W and Haaymann P W 1941 *Physica (Utrecht)* **8** 979
Verwey E J W, Haaymann P W and Romeijn F C 1947 *J. Chem. Phys.* **15** 181
Weiss P and Forrer R 1929 *Ann. Phys.* **12** 279
Whall T E, Rigo M O, Jones M R B and Poynton A J 1977 *J. Phys. (Paris)* **38** C1–229
Wu C and Mason T O 1981 *J. Am. Ceram. Soc.* **64** 520
Yamada Y 1975 *AIP Conf. Proc.* **24** 79
Yamada T, Suzuki K and Chikazumi S 1968 *Appl. Phys. Lett.* **13** 172
Yoshida J and Iida S 1979 *J. Phys. Soc. Jpn.* **47** 1627